



Contents lists available at ScienceDirect

## Neurobiology of Aging

journal homepage: [www.elsevier.com/locate/neuaging](http://www.elsevier.com/locate/neuaging)

## Fibrin deposited in the Alzheimer's disease brain promotes neuronal degeneration

Marta Cortes-Canteli, Larissa Mattei, Allison T. Richards, Erin H. Norris, Sidney Strickland\*

Patricia and John Rosenwald, Laboratory of Neurobiology and Genetics, The Rockefeller University, New York, NY, USA

### ARTICLE INFO

#### Article history:

Received 25 February 2014

Received in revised form 26 September 2014

Accepted 24 October 2014

#### Keywords:

Fibrinogen  
Alzheimer's disease  
Coagulation  
Neurodegeneration

### ABSTRACT

Alzheimer's disease (AD) is the most common form of dementia and has no effective treatment. Besides the well-known pathologic characteristics, this disease also has a vascular component, and substantial evidence shows increased thrombosis as well as a critical role for fibrin(ogen) in AD. This molecule has been implicated in neuroinflammation, neurovascular damage, blood-brain barrier permeability, vascular amyloid deposition, and memory deficits that are observed in AD. Here, we present evidence demonstrating that fibrin deposition increases in the AD brain and correlates with the degree of pathology. Moreover, we show that fibrin(ogen) is present in areas of dystrophic neurites and that a modest decrease in fibrinogen levels improves neuronal health and ameliorates amyloid pathology in the subiculum of AD mice. Our results further characterize the important role of fibrin(ogen) in this disease and support the design of therapeutic strategies aimed at blocking the interaction between fibrinogen and amyloid- $\beta$  (A $\beta$ ) and/or normalizing the increased thrombosis present in AD.

© 2014 Elsevier Inc. All rights reserved.

### 1. Introduction

Alzheimer's disease (AD) is a multifactorial and severe neurodegenerative disorder for which there is no effective treatment available (Huang and Mucke, 2012). The 2009 World Alzheimer Report estimated that 35.6 million people worldwide were affected by dementia in 2010 and predicted more than 100 million people by 2050 (Prince and Jackson, 2009). Therefore, new therapeutic approaches are sorely needed. This disorder has brain pathologic hallmarks such as amyloid- $\beta$  (A $\beta$ ) plaques and neurofibrillary tangles (Selkoe, 2011) and is characterized by a progressive reduction in cortical thickness and an overall decrease in brain volume with a loss of neurons (Duyckaerts et al., 2009; Gomez-Isla et al., 1996) and synapses (Terry et al., 1991). Besides the strong correlation with different vascular risk factors such as atherosclerosis, hypertension, hypercholesterolemia, and diabetes (de la Torre, 2002; Humpel, 2011), AD pathogenesis also involves cerebrovascular abnormalities such as alterations to the neurovascular unit (Iadecola, 2010) and decreases in cerebral blood flow (Austin et al., 2011; Mazza et al., 2011), suggesting that vascular disease influences AD pathogenesis (Kalaria et al., 2012).

Fibrinogen is a plasma glycoprotein that circulates at high concentration in the blood and is essential for coagulation as it is converted into fibrin in response to injury (Weisel, 2005). The balance between clot formation and degradation needs to be tightly regulated because alterations in this system can induce and exacerbate pathologic situations. Substantial evidence indicates a key role for fibrinogen and fibrin clot formation in AD pathogenesis. Increased fibrin(ogen) deposition is present in the brain parenchyma and brain vessels of human AD patients (Cortes-Canteli et al., 2010, 2012; Cullen et al., 2005; Fiala et al., 2002; Lipinski and Sajdel-Sulkowska, 2006; Ryu and McLarnon, 2009; Viggars et al., 2011) and mouse models of AD (Cortes-Canteli et al., 2010; Paul et al., 2007). However, most of these studies involved the immunohistochemical analysis of fibrin(ogen) in the AD brain using antibodies that fail to distinguish fibrinogen and fibrin (hence the use of the term fibrin(ogen)), making it impossible to know whether the deposits are composed of one or the other, or a mixture of the two. Fibrin(ogen) co-localizes with A $\beta$  in the AD brain (Cortes-Canteli et al., 2010, 2012; Jantaratnotai et al., 2010; Paul et al., 2007; Ryu and McLarnon, 2009), strongly interacts with this peptide (Ahn et al., 2010), and makes fibrin clots more difficult to degrade (Cortes-Canteli et al., 2010; Zamolodchikov and Strickland, 2012). AD mice are at high risk of arterial thrombosis (Jarre et al., 2014), and evidence indicates that there is increased obstruction of the cerebral blood vessels in the AD brain, which could strongly affect overall cerebral circulation. For example, aged ArcA $\beta$  AD mice have

\* Corresponding author at: Patricia and John Rosenwald, Laboratory of Neurobiology and Genetics, The Rockefeller University, 1230 York Avenue, New York, NY, 10065, USA. Tel.: +1 212 327 8705; fax: +1 212 327 8774.

E-mail address: [strickland@rockefeller.edu](mailto:strickland@rockefeller.edu) (S. Strickland).

increased occlusion of functional intracortical microvessels (Klohs et al., 2012). Similarly, TgCRND8 AD mice show evidence of increased clotting in their brains, and these fibrin clots are resistant to fibrinolysis (Cortes-Canteli et al., 2010). A prothrombotic state in AD patients is evidenced not only by increased clot formation but also by decreased fibrinolysis and elevated levels of activated coagulation factors and platelets (Cortes-Canteli et al., 2012). Indeed, reducing fibrinogen levels has beneficial effects in AD mice, such as decreasing blood-brain barrier permeability (Paul et al., 2007; Ryu and McLarnon, 2009), neurovascular damage (Paul et al., 2007), inflammation (Paul et al., 2007; Ryu and McLarnon, 2009), and cerebral amyloid angiopathy (Cortes-Canteli et al., 2010). This enhancement in vascular function likely improves cerebral blood flow and hence neuronal function and survival, leading to the amelioration of memory deficits observed in AD mice after fibrinogen reduction (Cortes-Canteli et al., 2010). However, no studies have shown direct evidence that the levels of fibrin(ogen) have an effect on neuronal viability and function. Here, we demonstrate that fibrin(ogen) is present in areas packed with dystrophic neurites and plays a key role in neuronal viability, because decreasing fibrinogen levels reduces the amount of neuronal loss, synaptic dysfunction, and amyloid pathology present in AD mice. We also report that insoluble fibrin accumulates in human and mouse AD brains and correlates with the degree of pathology. These results further characterize the role of fibrin(ogen) in AD pathophysiology and support the design of therapeutic strategies aimed at normalizing the irregular clotting observed in AD.

## 2. Methods

### 2.1. Mice

TgCRND8 mice express a double mutant form of the amyloid precursor protein 695 (KM670/671NL + V717F) (Chishti et al., 2001). These mice are on a mixed background (C57xCH3/C57) and develop age-dependent A $\beta$  pathology and memory deficits (provided by Drs M.A. Chishti and D. Westaway, University of Toronto, Canada). Four-, 15-, 58-, and 82-week-old TgCRND8 mice and their wild-type littermates ( $n = 3–7$  mice/group) were thoroughly perfused with saline heparin. Brains were removed, and one hemisphere was embedded, frozen in OCT, and processed for triple immunofluorescence analysis, whereas the cortex and hippocampus of the other hemisphere were dissected out and frozen for subsequent fibrin extraction.

Mice heterozygous for the *fibrinogen A $\alpha$  chain* ( $fbg^{+/-}$ ) (Suh et al., 1995) were crossed with TgCRND8 mice. TgCRND8;  $fbg^{+/-}$  mice and their littermate controls were thoroughly perfused with saline heparin, and brains were fixed in 4% paraformaldehyde, cryoprotected in 30% sucrose, frozen, and processed for NeuN, lysosomal-associated membrane protein-1 (LAMP-1), and Congo red determination.

All mice were genotyped twice, at time of weaning and at sacrifice. Mice were housed at The Rockefeller University's Comparative Biosciences Center and treated in accordance with IACUC-approved protocols.

### 2.2. Human samples

Human postmortem tissue was obtained from the Harvard Brain Tissue Resource Center. Blocks of frozen tissue from the superior frontal cortex ( $n = 4$  control and 15 AD cases), the anterior hippocampus with entorhinal cortex ( $n = 4$  control and 16 AD cases), and the hippocampal formation with parahippocampal gyrus ( $n = 8$  control and 29 AD cases) were sliced by cryostat (10- $\mu$ m sections)

for subsequent immunohistochemical analysis. Several sections were also collected in an Eppendorf tube for subsequent fibrin determination.

### 2.3. Fibrin extraction and Western blot

Mouse and human frozen tissue was homogenized in 5 volumes (g:mL) of phosphate-buffered saline (PBS) containing 1% Nonidet P-40, 0.5% sodium deoxycholate, 0.1% SDS, and protease inhibitor cocktail (Roche). The homogenate was centrifuged at 4 °C at 10,000g for 10 minutes, and the supernatant (soluble fraction) was transferred to a different tube. After several rounds of extraction, the insoluble (fibrin-containing) fraction was extracted as in Tabrizi et al. (1999) with slight modifications. Briefly, the pellet was homogenized in 3 M urea, vortexed for 2 hours at 37 °C, and centrifuged at 14,000g for 15 minutes. The supernatant was collected in a different tube, and the pellet was resuspended and vortexed at 65 °C for 30 minutes in reducing SDS loading buffer. Equal amounts were run on a 4%–20% gradient polyacrylamide Criterion gel (Bio-Rad), transferred to a polyvinylidene fluoride membrane (Pall), and incubated with the following antibodies: rabbit polyclonal anti-fibrin(ogen) antibody (gift from Dr J. L. Degen, Cincinnati, OH, USA), mouse monoclonal anti-fibrin antibody (59D8; (Hui et al., 1983), gift from Dr T. Renne, Karolinska Institutet, Sweden), mouse monoclonal anti-A $\beta$  antibody (6E10, Covance), and rat monoclonal anti-tubulin antibody (YOL1/34, Abcam). Tubulin was used as loading control because it is present in different fractions after sequential solubilization steps and extensive rounds of extraction in the rat brain (Schindler et al., 2006). In vitro human or mouse fibrin clots were prepared as positive controls (Cortes-Canteli et al., 2010; Zamolodchikov and Strickland, 2012) and run in parallel with the samples. Samples were subjected to Western blot analysis 4–5 different times. Fibrin  $\beta$ -chain and tubulin bands were quantified using NIH Image J 1.46o software, and the ratio of fibrin:tubulin was plotted on a graph.

### 2.4. Human brain staining

Frozen human AD and control brain sections (10  $\mu$ m) were fixed in 4% paraformaldehyde and treated with proteinase K (Dako) before performing the following staining protocols.

Fibrin immunohistochemistry: sections were immersed in methanol/H<sub>2</sub>O<sub>2</sub> to inactivate endogenous peroxidases, blocked in Tris buffer with 2% donkey:horse serum (1:1), and incubated overnight with the mouse monoclonal antibody 59D8 that specifically detects human fibrin (Hui et al., 1983). The following morning, sections were incubated with a biotinylated horse anti-mouse antibody, amplified by the VECTASTAIN Elite ABC Ready-to-Use Reagent, and developed using ImmPACT DAB Peroxidase Substrate (all from Vector Laboratories). Sections were then dehydrated, mounted, and imaged using a Zeiss Axiovert 200 microscope.

Triple immunofluorescence: sections were blocked in Tris buffer with 2% goat serum followed by overnight incubation with a mouse monoclonal anti-human LAMP-1 antibody (clone H4A3, Developmental Studies Hybridoma Bank) and a rabbit polyclonal anti-human fibrinogen antibody (Dako). Then, the sections were incubated for 1 hour at RT with the highly cross-adsorbed secondary fluorescent antibodies CF405M goat anti-rabbit and CF555 goat anti-mouse (Biotium), rinsed, and incubated overnight with anti-A $\beta$  monoclonal antibody 6E10 labeled with Alexa Fluor 488 (Covance). The tissue was incubated with 0.3% Sudan Black B in 70% ethanol to block lipofuscin autofluorescence and finally covered with Vectashield (Vector Laboratories). Secondary controls omitting primary antibodies as well as controls using each individual primary antibody alone were carried out in parallel. An inverted TCS SP8 laser scanning

confocal microscope (Leica) equipped with a fully tunable white light laser, a 405 nm laser, 3 HyD detectors, and an HCX PL APO CS 40.0x1.10 water objective, available at The Rockefeller University Bio-Imaging Resource Center, was used to acquire the images. Sixteen bit images of areas rich in amyloid were taken sequentially at 1024 × 1024, at 600 Hz scan speed and keeping laser and exposure conditions constant in all 3 channels. An average of 3–4 pictures per section was taken, and the percentage of colocalization between the different markers was analyzed using MetaMorph software (Molecular Devices). The region of interest, comprised A $\beta$  staining, was marked, and then images were separated into the 3 channels (blue, green, and red), thresholded, and transformed to binary. The total number of pixels in each of these original binary images was recorded. Images were then combined using “logical AND,” first in pairs (blue-green, blue-red, and green-blue) and then in a trio (blue-green-red). The resulting binary images show only those pixels positive in the combined channels; and therefore, the percentage of colocalization and tri-localization was calculated by comparing these with the total number of pixels in each of the original binary images.

### 2.5. Mouse brain staining

**Triple immunofluorescence:** frozen coronal sections (20  $\mu$ m) from 4-, 15-, 58-, and 82-week-old TgCRND8 mice and their wild-type littermates ( $n = 3–8$  mice/group) were fixed in cold ethanol and treated for 2 minutes with Proteinase K (Dako) diluted 1:4 in Tris buffer. Fibrin(ogen) immunohistochemistry was performed using a rabbit polyclonal biotinylated anti-fibrin(ogen) antibody (Abcam) and the Tyramide Signal Amplification system (Perkin Elmer), according to manufacturer’s instructions. A control using biotinylated rabbit IgG in place of anti-fibrin(ogen) antibody was included to verify the specificity of the antibody. Fibrin(ogen) was visualized using CF405M streptavidin (Biotium). Sections then were blocked for 1 hour in PBS containing 0.25% Triton X-100 and 3% goat serum (Vector Laboratories) and incubated overnight at 4 °C with rat monoclonal anti-mouse LAMP-1 antibody (clone 1D4B, Developmental Studies Hybridoma Bank) and 6E10 Alexa Fluor 488-conjugated anti-A $\beta$  mouse monoclonal antibody (Covance). Sections were then incubated for 2 hours with Alexa Fluor 594 goat anti-rat secondary antibody and coverslipped with Vectashield (Vector Laboratories). Secondary controls omitting primary antibodies as well as controls using each individual primary antibody alone were carried out in parallel. Images from the cortex and hippocampus were taken and quantified as described previously for the triple immunofluorescence performed in human sections.

**NeuN immunohistochemistry and quantification:** floating-coronal sections (20  $\mu$ m) from 82-week-old TgCRND8;  $fbg^{+/+}$  mice, TgCRND8;  $fbg^{+/-}$  mice, and their wild-type littermate controls ( $n = 3–7$  mice/group) were processed for immunohistochemistry using a mouse monoclonal NeuN antibody (Chemicon) to identify neurons. The Vector Mouse-on-Mouse kit (Vector Laboratories) was used according to the manufacturer’s instructions to decrease nonspecific staining because of endogenous immunoglobulins. The diaminobenzidine method was used for development. Counterstaining with 0.5% Thioflavin S (Sigma) was performed to identify amyloid (not shown). Low magnification images were captured to identify the corresponding Bregma of each section analyzed. High magnification images of the entire dorsal subiculum area were taken using a 20 $\times$  objective to avoid oversampling errors. The dorsal subiculum is adjacent to the CA1 layer and expands from Bregma  $-2.54$  mm to  $-3.80$  mm (Franklin and Paxinos, 2008). Because its shape, size, and structure change substantially along its anatomy, we focused our study on the central region of the dorsal subiculum. NeuN-positive cells were quantified in every approximately fourth coronal section

covering the unilateral dorsal subiculum from Bregma  $-2.7$  mm to  $-3.4$  mm. The total number of NeuN-positive cells and the area analyzed were measured in each section using Image J. A total of 160 sections (approximately 8 sections/mouse) were analyzed, averaged per group, and plotted relative to the wild-type control. To avoid differences in neuronal density among the different Bregmas, the average of analyzed sections per mouse and per group was maintained at Bregma  $-3.0$  mm.

**Lamp-1 and Congo red staining and quantification:** floating-coronal sections (20  $\mu$ m) from 82-week-old TgCRND8;  $fbg^{+/+}$  and TgCRND8;  $fbg^{+/-}$  mice were washed in PBS, blocked for 1 hour in PBS containing 0.25% Triton X-100 and 3% goat serum (Vector Laboratories), and incubated overnight at 4 °C with rat monoclonal anti-mouse LAMP-1 antibody (clone 1D4B, Developmental Studies Hybridoma Bank) and mouse monoclonal anti-NeuN antibody. Sections were then incubated for 2 hours with Alexa Fluor 488 goat anti-rat and Alexa Fluor 647 goat anti-mouse secondary antibodies (Invitrogen), mounted, and counterstained with 0.2% Congo red (Sigma) dissolved in 70% isopropanol. Sections were coverslipped with Vectashield and imaged using an inverted Leica TCS SP5 laser scanning confocal microscope equipped with a fully tunable white light laser, 2 HyD detectors, 1 PMT detector, and a super-Z stage for rapid tiling, available at The Rockefeller University Bio-Imaging Resource Center. Z-stack tile-scans covering the subicular area (identified by NeuN staining) were acquired in all 3 channels using an HCX PL APO CS 40.0x1.10 water objective. Twelve bit images were taken at 1024 × 1024, at 600 Hz scan speed. Laser and exposure conditions were kept constant between genotypes. Reconstructed tile-scan images were thresholded in Image J, and the LAMP-1- and Congo red-positive areas were quantified in each individual plane. The total LAMP-1- and Congo red-positive areas in the subiculum were then calculated in each section, averaged, and compared between groups.

### 2.6. Statistics

All numerical values are presented as mean  $\pm$  standard error of the mean. Statistical analysis in human samples was performed using the nonparametric Mann-Whitney test. Statistical significance in mouse samples was determined using 2-tailed  $t$  test analysis comparing the different experimental groups. Two-way analysis of variance and Bonferroni posttest were also performed to determine whether the effect of genotype and treatment were considered significant.  $p$ -values  $< 0.05$  were considered significant.

## 3. Results

### 3.1. Fibrin is present in the AD brain and correlates with the degree of pathology

Fibrin(ogen) is abnormally deposited in the AD brain. It is important to know whether these deposits are composed of fibrinogen, fibrin, or a mixture of the two. It is also critical to understand whether fibrin(ogen) accumulation correlates with the degree of AD pathology and to quantify the actual level of fibrin(ogen) deposition compared with controls. To that end, we extracted the insoluble protein fraction, where fibrin is located (Tabrizi et al., 1999), from different regions of human postmortem brain samples and compared nondemented controls with AD patients. As shown in top panels of Fig. 1A–C, fibrin is present in the brains of human AD patients. The main product detected, fibrin- $\beta$  chain at approximately 52 kDa, is significantly increased in AD samples in all the areas of the brain analyzed compared with nondemented control samples (Fig. 1D–F). As expected, control patients present with very low amounts of insoluble fibrin in the brain. We detected more than

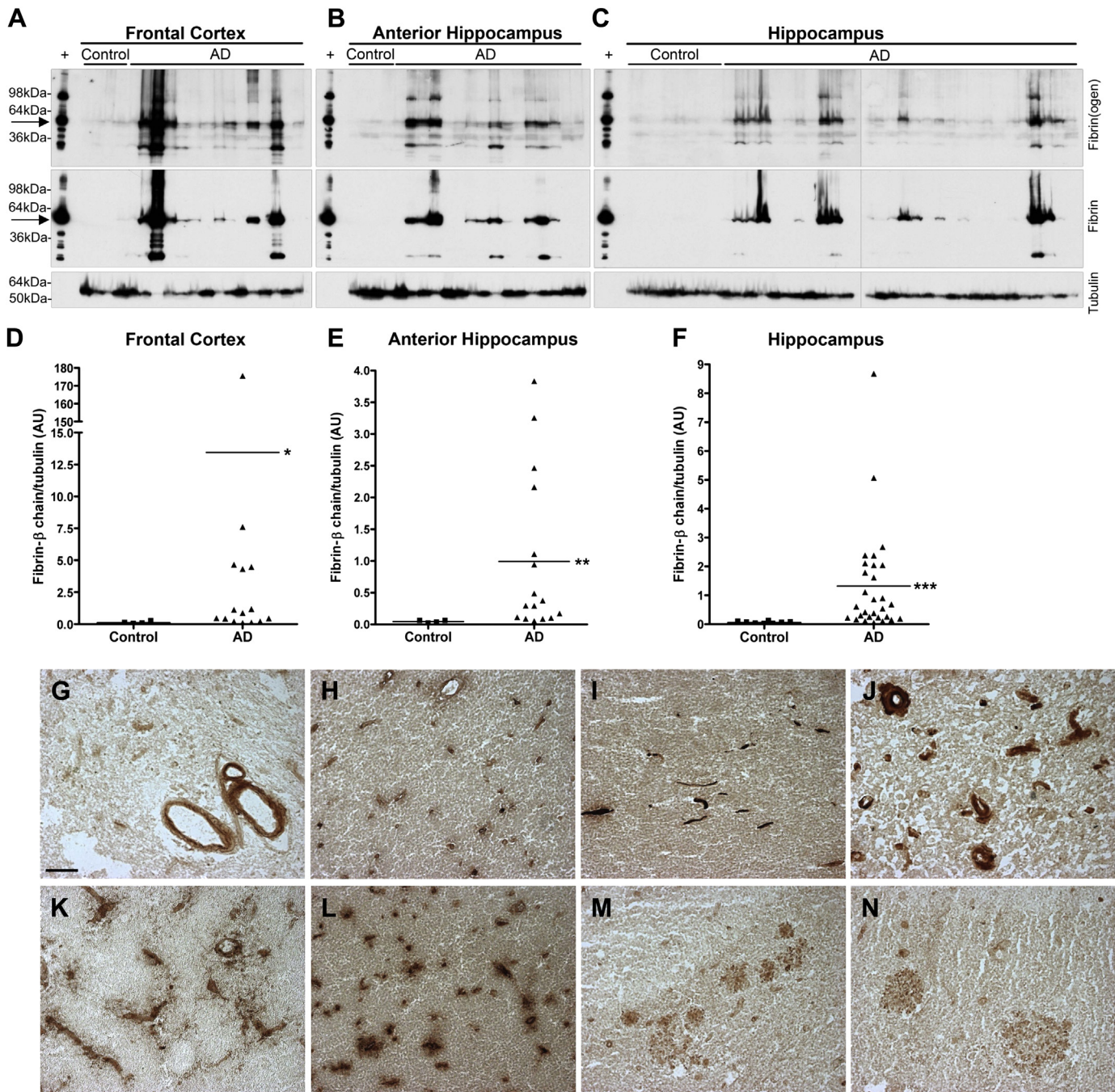


**Fig. 1.** Fibrin deposition is increased in the human AD brain. Fibrin was isolated from the superior frontal cortex (A and D; n = 4 control and 15 AD), the anterior hippocampus with entorhinal cortex (B and E; n = 4 control and 16 AD), and the hippocampal formation with parahippocampal gyrus (C and F; n = 8 control and 29 AD) of postmortem samples from AD patients and nondemented control subjects. The insoluble fibrin-containing fraction was extracted and analyzed by Western blot. Fibrin was detected with an anti-fibrin(ogen) polyclonal antibody (top panels) or an anti-fibrin monoclonal antibody (59D8; (Hui et al., 1983); middle panels). Blots were reprobated with anti-tubulin antibody as loading control (bottom panels). Soluble fibrinogen is not present in these samples because it was removed during the extraction process. Each lane corresponds to an individual patient. Samples were run 4 different times, quantified, averaged, and plotted. Fibrin  $\beta$ -chain (approximately 52 kDa, arrows) was significantly increased in AD brains compared with nondemented control subjects in all regions analyzed (D–F). An *in vitro* fibrin clot prepared with human fibrinogen was run as positive control (+). Hippocampal samples were run on different gels because of space limitations (separated by a vertical line in C), and 4–6 samples were run on both gels to ensure results were similar between gels. Graphs show mean and Mann-Whitney test \* $p < 0.05$ , \*\* $p < 0.01$ , and \*\*\* $p < 0.001$  comparing AD versus control. Fibrin immunohistochemistry was performed on human AD hippocampal cryosections using the 59D8 antibody and the same set of patients used in C. Fibrin was found intravascularly, lining big vessels (G) and/or blocking small ones (H–J), as well as extravascularly, in the vicinity of blood vessels (K and L) or forming plaque-like structures (M and N). Each image corresponds to a different human AD patient. Scale bar, 50  $\mu$ m. Abbreviation: AD, Alzheimer's disease.

a 100-fold increase in fibrin deposition in the superior frontal cortex (Fig. 1D,  $0.12 \pm 0.05$  control vs.  $13.45 \pm 11.6$  AD; \* $p < 0.05$ ), a 23-fold increase in the anterior hippocampus (Fig. 1E,  $0.04 \pm 0.01$  control vs.  $0.99 \pm 0.3$  AD; \*\* $p < 0.01$ ), and more than a 20-fold

increase in the hippocampus (Fig. 1F,  $0.06 \pm 0.01$  control vs.  $1.3 \pm 0.3$  AD; \*\*\* $p < 0.001$ ) of AD patients compared with nondemented control subjects. We reprobated the membrane with a specific monoclonal antibody against human fibrin, clone 59D8 (Hui et al.,

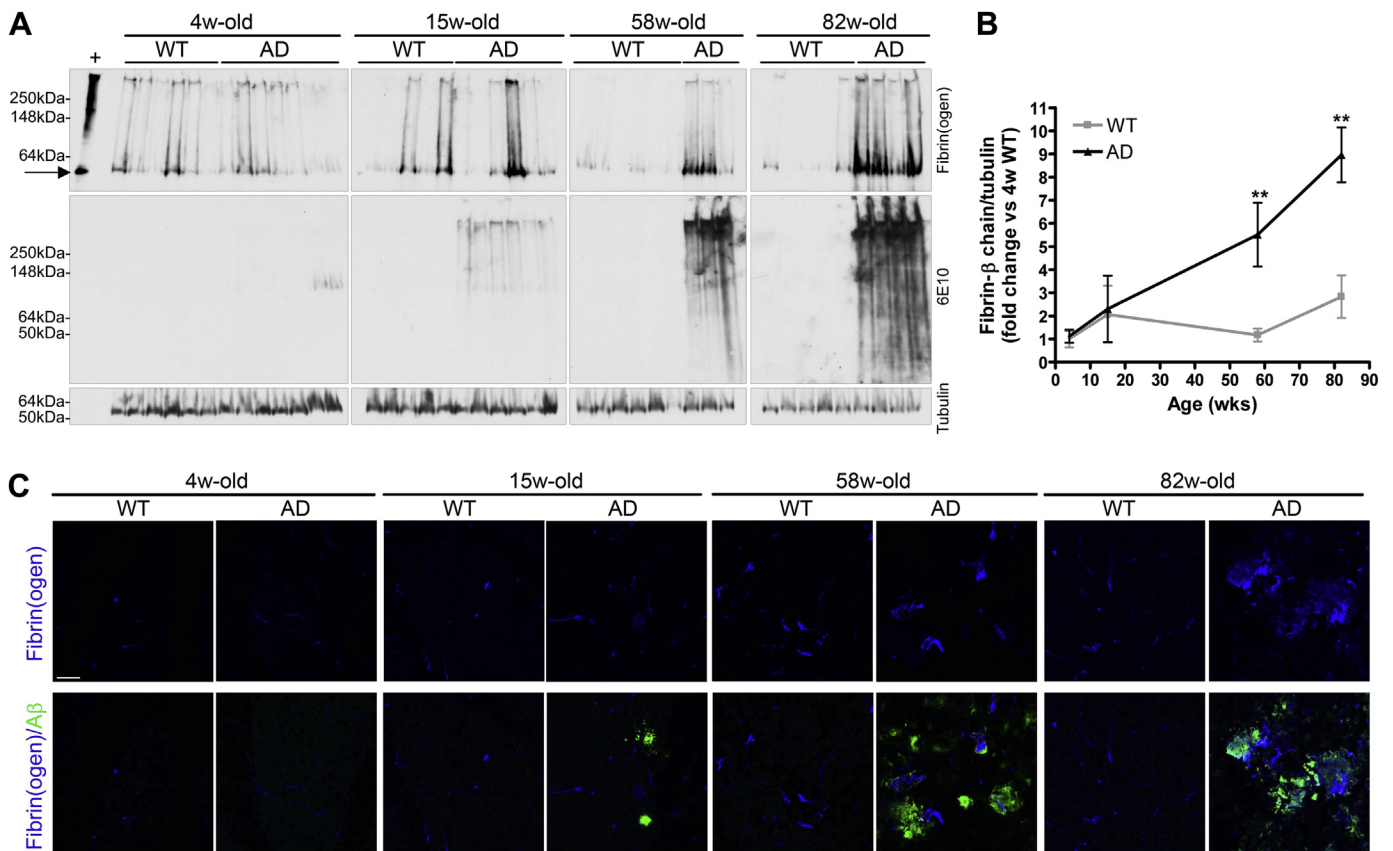


**Fig. 2.** Fibrin deposition is increased in the brains of AD mice and correlates with A $\beta$  pathology. (A) To detect fibrin deposited in the mouse brain, we used cortical and hippocampal samples from 4-, 15-, 58- and 82-week-old TgCRND8 mice (AD) and their wild-type (WT) littermate controls ( $n = 3-7$ /group). The insoluble (fibrin-containing) fraction was extracted, analyzed by Western blot, and probed with antibodies specific for murine fibrin(ogen) (top panels). Fibrinogen immunoreactivity was not detected because soluble fibrinogen was removed during the extraction protocol. The blots were reprobed with 6E10 antibody to detect A $\beta$  pathology (middle panels) and with anti-tubulin antibody as loading control (bottom panels). Each lane corresponds to an individual mouse. Samples were run 5 times, quantified, averaged, and plotted by age and genotype. (B) Quantification indicates that the amount of fibrin  $\beta$ -chain (approximately 52 kDa, arrow in A) is significantly increased in the brains of 58- and 82-week-old AD mice compared with their littermate controls. This increase in fibrin deposition correlates with A $\beta$  pathology. An *in vitro* fibrin clot prepared with mouse fibrinogen was used as positive control (+). Graph shows mean  $\pm$  SEM and Student *t* test  $**p < 0.01$  comparing AD versus WT. Two-way ANOVA and Bonferroni posttest analysis also showed the effect of genotype ( $p = 0.0003$ ) and age ( $p = 0.0001$ ) are significant. (C) Double immunofluorescence was performed on the same set of TgCRND8 mice and WT littermates used in A. Representative confocal images from the cortex and hippocampus show that fibrin(ogen) (blue) and A $\beta$  (green) staining increase with age and co-localize in the AD mouse brain. Scale bar, 40  $\mu$ m. Abbreviations: A $\beta$ , amyloid- $\beta$ ; AD, Alzheimer's disease; ANOVA, analysis of variance; SEM, standard error of the mean.

1983) and obtained similar results (Fig. 1A–C, middle panels), confirming that most soluble fibrinogen was indeed removed during the extraction protocol, and we are detecting mostly insoluble fibrin. The membranes were reprobed with a tubulin antibody as loading control (Fig. 1A–C, bottom panels). The intermediate fractions generated during this extraction protocol (the soluble and urea supernatant fractions) were also analyzed (data not shown). No fibrin was detected in any of those fractions, confirming that fibrin was not lost in any steps of the protocol and that all the fibrin deposited in the brain was being detected.

We next analyzed the localization of fibrin in the set of AD patients that presented with high levels of this protein deposited in the hippocampus (Fig. 1C). Immunohistochemical analysis revealed different patterns of fibrin distribution. Some of the AD patients analyzed presented fibrin exclusively within the vasculature, lining big vessels (Fig. 1G), blocking capillaries (Fig. 1H and I), or a combination of both (Fig. 1J). Other AD patients showed fibrin extravasated as perivascular leakage “clouds” (Fig. 1K and L) or into the brain parenchyma (Fig. 1M and N).

To analyze the amount of fibrin in a more uniform system, we used AD mice. Although AD mouse models do not fully recapitulate the human disease, they are more homogenous than humans and

allow for a better in-depth analysis of specific components because they accumulate A $\beta$  and develop pathology as they age. We examined the amount of fibrin present in the cortex and hippocampus of TgCRND8 AD mice (Chishti et al., 2001) at 4, 15, 58, and 82 weeks (Fig. 2), ages that correspond to different stages of AD pathology (Chishti et al., 2001). As previously described for human brain tissue, we extracted and analyzed the insoluble fractions by Western blot. We observed low amounts of fibrin- $\beta$  chain in the brains of 4-week-old mice, when no A $\beta$  pathology was present. However, the amount of fibrin significantly increased in the brains of 58- and 82-week-old AD mice compared with their age-matched wild-type littermates (Fig. 2A, upper panels, and B). Moreover, this significant increase in fibrin appeared to correlate with A $\beta$  pathology, as detected by the 6E10 antibody (Fig. 2, middle panels). The membranes were reprobed with a tubulin antibody as loading control (Fig. 2, bottom panels). Unfortunately, the human-specific fibrin antibody 59D8 recognized mouse fibrin very weakly in the positive control (data not shown) and therefore could not be used to properly detect fibrin in these specimens. To identify where this fibrin deposition was taking place, we performed immunostaining in the same set of TgCRND8 mice. Double immunofluorescence showed that fibrin(ogen) and A $\beta$  increase with age in the AD brain,

reproducing the results obtained in Fig. 2A, and that fibrin(ogen) deposits co-localize with A $\beta$  in amyloid plaques (Fig. 2C).

Overall, these results demonstrated that fibrin, the main protein component of blood clots, accumulates in the human and mouse AD brain where it appears to correlate with the degree of A $\beta$  pathology.

### 3.2. Fibrin(ogen) is present in areas of dystrophic neurites and amyloid pathology in the AD brain

We investigated whether fibrin(ogen) is present in areas of synaptic dysfunction, one of the first and most important pathologic hallmarks of AD that correlates very well with cognitive decline (Terry et al., 1991). Because lysosomes and other autophagy-related organelles are part of the neuritic dystrophy observed in AD (Lee et al., 2011; Nixon et al., 2005), we stained for LAMP-1 to identify areas of synaptic dysfunction. This marker is highly up-regulated in the human AD brain (Barrachina et al., 2006) and cerebrospinal fluid (Armstrong et al., 2014), as well as highly enriched in the dystrophic areas surrounding amyloid plaques in AD mice (Condello et al., 2011; Hashimoto et al., 2010) and human AD patient brains (Barrachina et al., 2006; Perez-Gracia et al., 2008). Human postmortem hippocampal sections were co-stained for fibrin(ogen), LAMP-1, and A $\beta$  (Fig. 3A). Fibrin(ogen) was present in areas of dystrophic neurites along with A $\beta$  deposition. Several

patterns of fibrin(ogen) deposition were found in the different AD patients. Fibrin(ogen) was present in the core of fibrillar plaques (arrows in AD patient 1, Fig. 3A), diffuse amyloid (arrowheads in AD patient 1, Fig. 3A) and was also found co-localized with A $\beta$  staining and areas of synaptic dysfunction in the vicinity of blood vessels (arrow in AD patient 2, Fig. 3A). Confocal analysis and subsequent quantification revealed that 16.7% ( $\pm 4.1$ ) of the fibrin(ogen) staining present in amyloid areas in the human AD brain was co-localized with A $\beta$  and 37.1% ( $\pm 4.6$ ) with LAMP-1. The amount of fibrin(ogen) co-localized with both markers had an average of 9.7% ( $\pm 2.2$ ) overlap of pixels from all 3 molecules, with a maximum in some areas of 49.9% tri-localization. Nevertheless, it should be emphasized that the 3 markers do not need to be fully overlapping to impact each other's function and play a role in AD pathophysiology. For example, fibrin(ogen) is a strong proinflammatory molecule (Davalos and Akassoglou, 2012), and therefore its presence in abnormal deposits in or around amyloid plaques could exacerbate the inflammatory response already present in AD and promote neuronal dysfunction (Solito and Sastre, 2012). To do this, fibrin(ogen) does not need to be co-localized with these markers but rather be in the same area.

We next investigated whether the abnormal accumulation of fibrin(ogen) present in the AD mouse brain (Fig. 2) coincided with areas of synaptic dysfunction. Triple immunofluorescence analysis

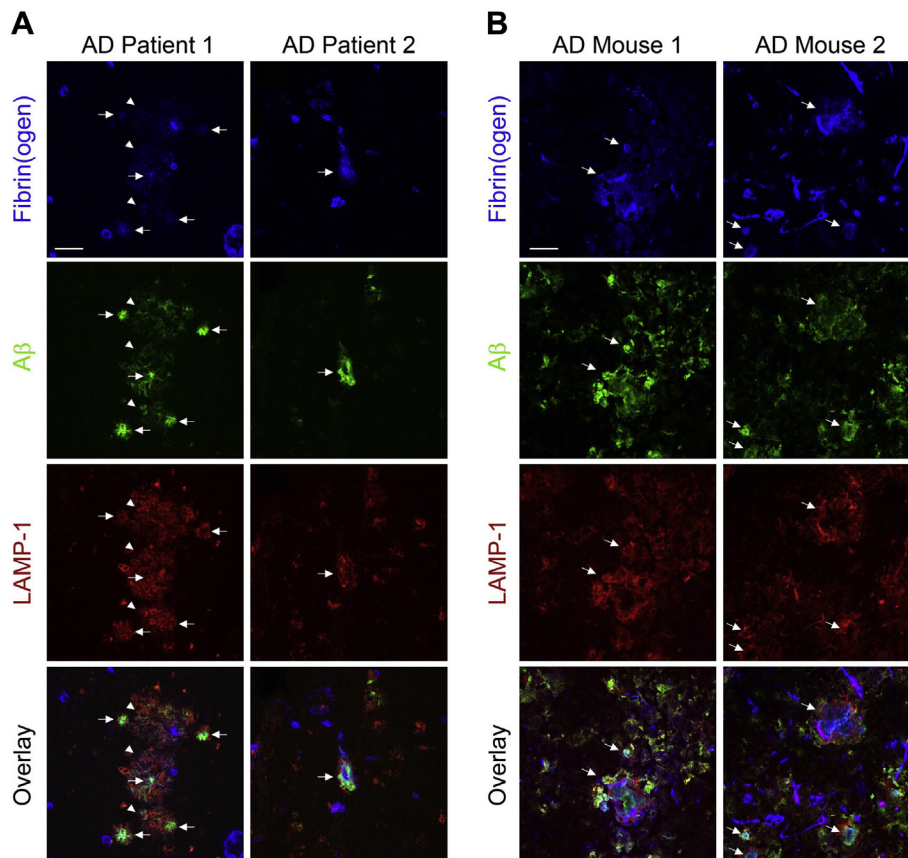


**Fig. 3.** Fibrin(ogen) extravasation is present in areas of synaptic dysfunction in the human and mouse AD brain. (A) Postmortem hippocampal sections from AD patients were stained with an anti-fibrin(ogen) antibody (blue) in combination with anti-A $\beta$  (green) and anti-LAMP-1 (red) antibodies to detect amyloid pathology and dystrophic neurites, respectively. Several patterns of fibrin(ogen) staining were found in the different human AD cases. Fibrin(ogen) co-localized with LAMP-1 in the core of amyloid plaques (arrows in AD patient 1) but also with diffuse A $\beta$  (arrowheads in AD patient 2). Fibrin(ogen) was also found in areas of synaptic dysfunction and amyloid pathology close to blood vessels (arrow in AD patient 2). Images correspond to 2 different human AD patients. Scale bar, 40  $\mu$ m. (B) Immunofluorescent analysis of fibrin(ogen) (blue) in combination with dystrophic neurites (LAMP-1, red) and A $\beta$  pathology (6E10, green) was performed on brain samples from 82-week-old TgCRND8 AD mice. A similar pattern throughout the brain was found in the AD mice with strong fibrin(ogen) staining in LAMP-1 and A $\beta$ -positive areas (arrows). Representative images of the staining from 2 different 82-week-old TgCRND8 mice are shown. Scale bar, 40  $\mu$ m. Abbreviations: A $\beta$ , amyloid- $\beta$ ; AD, Alzheimer's disease.

showed that fibrin(ogen) accumulated in areas rich in LAMP-1 as well as A $\beta$  staining in the brains of 82-week-old TgCRND8 AD mice (Fig. 3B). The accumulation pattern was more homogenous than what was found in the human AD brain, with most of the fibrin(ogen) observed in patches that often coincided with areas of dystrophic neurites as well as A $\beta$  pathology (arrows in Fig. 3B). Quantification analysis showed that 29.6% ( $\pm 6.2$ ) of fibrin(ogen) staining present in amyloid areas co-localized with A $\beta$  and 36.1% ( $\pm 5.8$ ) with LAMP-1. The percentage of pixels with tri-localization had an average of 13.3% ( $\pm 2.7$ ), with a maximum in some areas of 53.8% tri-localization.

These results provide further evidence that fibrin(ogen) is not only abnormally present in the AD brain colocalizing with A $\beta$  but is also found in areas fully packed with dystrophic neurites.

### 3.3. Decreasing fibrinogen levels reduces neuronal death in the dorsal subiculum of AD mice

Because significant amounts of fibrin are found in the AD mouse brain (Fig. 2), and fibrin(ogen) is present in areas of synaptic dysfunction and A $\beta$  pathology (Fig. 3), we investigated whether modulating fibrinogen levels could affect the characteristic loss of neurons present in AD. Although most of the AD mouse models do not present robust and widespread neuronal death as the human AD brain does (Duyckaerts et al., 2008; Gomez-Isla et al., 1996), localized neurodegeneration has been reported in some AD mouse lines (Wirhth and Bayer, 2010) in areas such as the subiculum (Oakley et al., 2006). The subiculum is a relatively well-defined structure of the hippocampus that plays an essential role in memory processing (O'Mara, 2005) and is profoundly affected in AD (Falke et al., 2003). Immunohistochemical analysis using the specific neuronal marker NeuN showed a dramatic reduction in the number of neurons present in the dorsal subiculum of 82-week-old TgCRND8 AD mice (Fig. 4A vs. C). We quantified the extent of neuronal loss in this area, revealing that 82-week-old TgCRND8 mice have approximately 25% fewer subicular neurons than their wild-type littermates (Fig. 4E). This result is in line with stereological studies performed on the human AD hippocampus (Zilkova et al., 2006).

We then determined whether reducing fibrinogen levels could affect neuronal health in TgCRND8 mice. We used TgCRND8 mice heterozygous for a mutation in the *fibrinogen*  $\alpha$ -chain gene, TgCRND8; *fbg*<sup>+/-</sup> mice, that have an approximately 30% decrease in fibrinogen levels (Suh et al., 1995). We focused our studies on 82-week-old TgCRND8; *fbg*<sup>+/-</sup> mice because fibrin levels peaked at that age (Fig. 2). NeuN immunohistochemistry and subsequent quantification showed that AD mice with only 1 copy of the *fibrinogen* gene had significantly more neurons in the dorsal subiculum than AD littermate controls (Fig. 4C vs. D and E; 73.3%  $\pm$  1.7% TgCRND8; *fbg*<sup>+/+</sup> mice versus 78.2%  $\pm$  1.3% TgCRND8; *fbg*<sup>+/-</sup> mice; \**p* < 0.05). Bearing 1 copy of the *fibrinogen* gene did not affect the overall amount of neurons in the subiculum of wild-type littermates (Fig. 4A vs. B and E). These results indicate that fibrinogen levels affect the neuronal loss observed in the AD mouse brain.

### 3.4. Decreasing fibrinogen levels ameliorates synaptic dysfunction and amyloid pathology in the subiculum of AD mice

Because neuronal loss is accompanied by a reduction in synapses, we investigated if reducing fibrinogen levels could ameliorate the degree of synaptic dysfunction in the AD brain. As in Fig. 3, we used LAMP-1 as a marker of dystrophic neurites because it provides an excellent contrast with the surrounding tissue (Condello et al., 2011) and thus allows for quantification of the dystrophic area. In addition to LAMP-1, we co-stained brain sections with anti-NeuN antibody to identify the dorsal subiculum and with Congo red to detect amyloid plaques. We acquired high resolution confocal Z-stack tile-scans covering the subicular area in all 3 channels (Fig. 5A–F). The total LAMP-1-positive area was quantified within the subiculum and compared between 82-week-old TgCRND8; *fbg*<sup>+/+</sup> mice and TgCRND8; *fbg*<sup>+/-</sup> mice. We found a 25% decrease in the amount of dystrophic neurites in the dorsal subiculum of AD mice with just 1 copy of the *fibrinogen* gene (Fig. 5G; 100%  $\pm$  10.7% TgCRND8; *fbg*<sup>+/+</sup> mice vs. 74.5%  $\pm$  7% TgCRND8; *fbg*<sup>+/-</sup> mice; \**p* < 0.05). We also observed that reducing fibrinogen levels provoked a marked reduction in the amount of amyloid pathology present in that area (Fig. 5H; 100%  $\pm$  11.6% TgCRND8; *fbg*<sup>+/+</sup> mice vs. 58.2%  $\pm$  5.9% TgCRND8; *fbg*<sup>+/-</sup> mice; \*\**p* < 0.01). These results indicate that

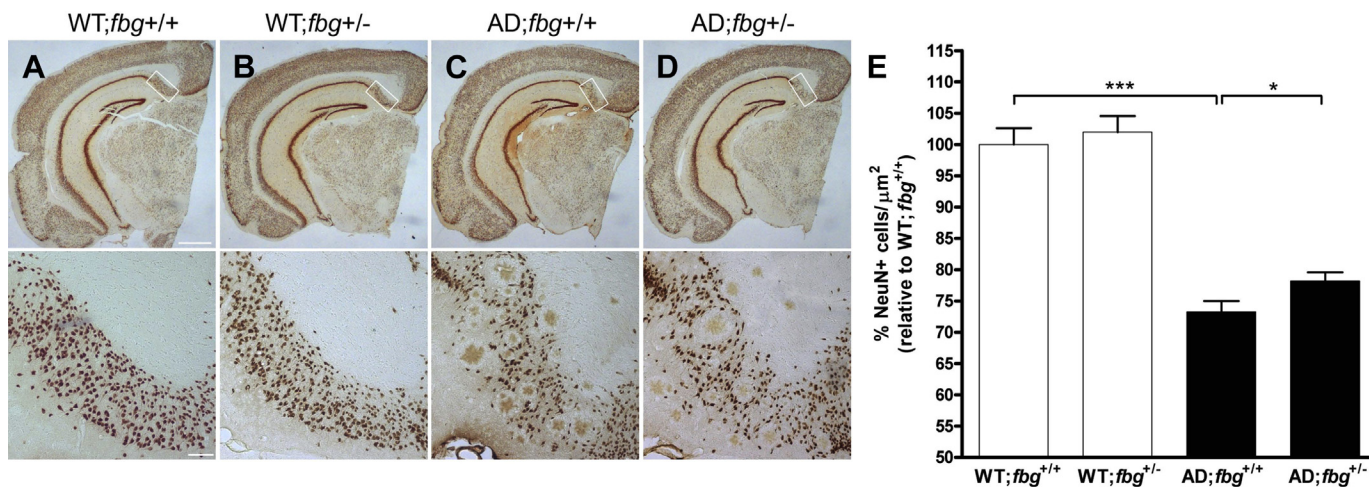


**Fig. 4.** Decreasing fibrinogen levels ameliorates neuronal death in AD mice. Neuronal death was analyzed in TgCRND8 mice (AD; *fbg*<sup>+/+</sup>), TgCRND8 mice heterozygous for a mutation in the *fibrinogen*  $\alpha$ -chain gene (AD; *fbg*<sup>+/-</sup>), and their corresponding wild-type littermates (WT; *fbg*<sup>+/+</sup> and WT; *fbg*<sup>+/-</sup>). NeuN immunohistochemical analysis was performed to determine the number of neurons (A–D). The total number of NeuN-positive cells in the subiculum (boxed area, higher magnification in bottom panels) was quantified as explained in Section 2. (E) Graph represents the percentage of neurons per  $\mu\text{m}^2$  analyzed relative to WT; *fbg*<sup>+/+</sup> mice. AD; *fbg*<sup>+/+</sup> mice have significantly more neuronal death in the subiculum compared with WT controls, whereas AD; *fbg*<sup>+/-</sup> mice have significantly less neuronal death in this area of the brain compared with AD; *fbg*<sup>+/+</sup> mice. (n = 3–7 mice/group, approximately 8 sections/mouse). Average Bregma analyzed was kept at  $-3.0$  mm per group and per mouse. Graph shows mean  $\pm$  SEM and Student t test \*\*\**p* < 0.001; \**p* < 0.05. Scale bars, 500  $\mu\text{m}$  (top panels) and 50  $\mu\text{m}$  (bottom panels). Abbreviations: AD, Alzheimer's disease; SEM, standard error of the mean.

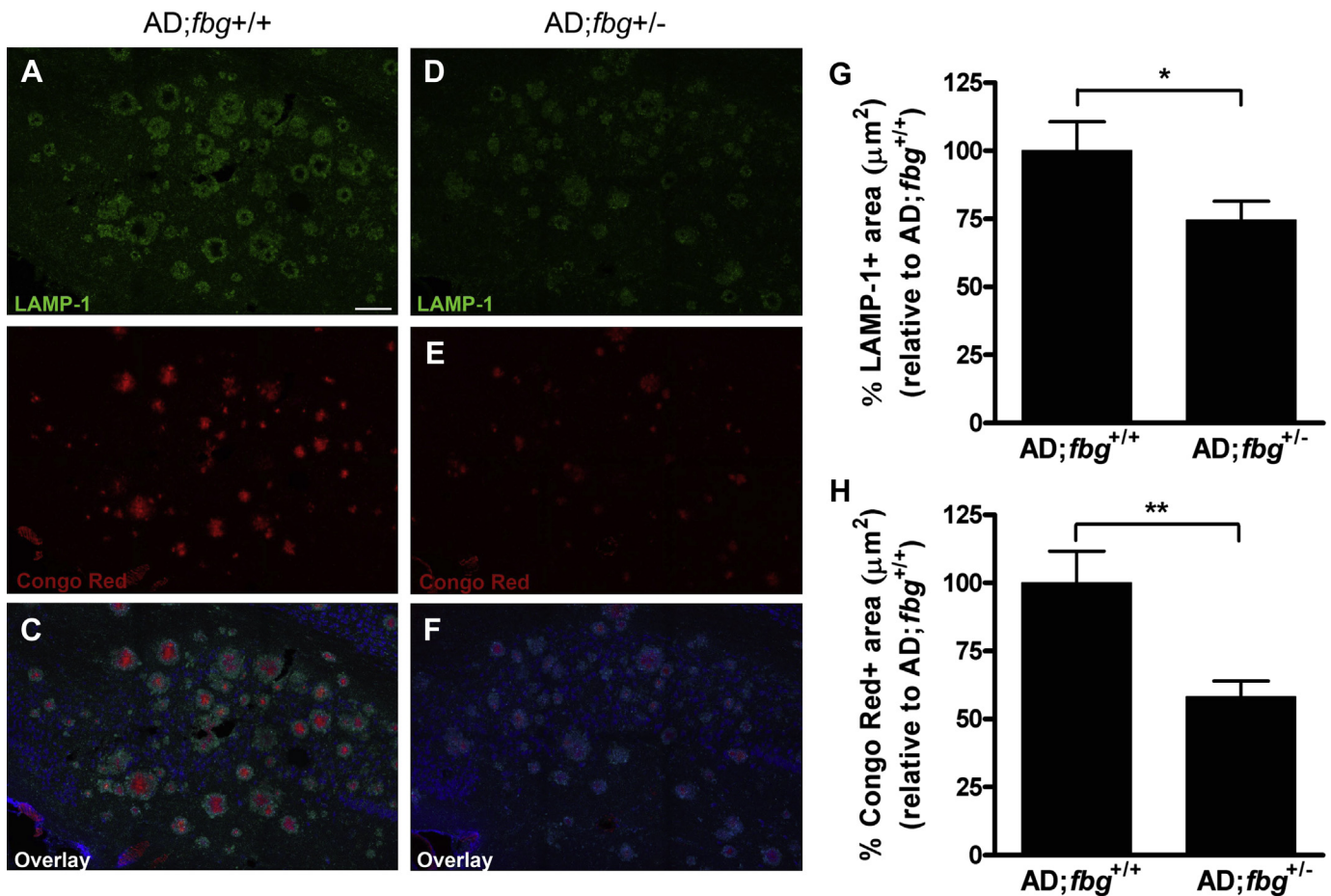


**Fig. 5.** Decreasing fibrinogen levels reduces synaptic dysfunction and amyloid pathology in AD mice. Triple staining was performed on sections from TgCRND8 AD mice (AD; *fbg*<sup>+/+</sup>) and AD mice heterozygous for a mutation in the *fibrinogen A $\alpha$ -chain* gene (AD; *fbg*<sup>+/-</sup>). Anti-LAMP-1 antibody (A and D, green) and Congo red staining (B and E, red) were used to identify dystrophic neurites and amyloid pathology, respectively. Sections were also analyzed with anti-NeuN antibody to observe neuronal bodies and identify the area of the subiculum (C and F, blue). Confocal Z-stacks of the subicular area were taken in all 3 channels, keeping constant conditions between groups. Each individual plane was quantified using NIH Image J software. Representative maximum projection tile-scan images are shown. Graphs represent the percentage of LAMP-1- (G) or Congo red- (H) positive area versus the total subicular area analyzed, relative to the AD group. AD; *fbg*<sup>+/-</sup> mice presented a significant reduction in the amount of synaptic dysfunction as well as amyloid pathology in the subiculum (n = 2–4 mice/group, 2–3 sections/mouse). Graph shows mean  $\pm$  SEM and Student *t* test \*\**p* < 0.01; \**p* < 0.05. Scale bar, 100  $\mu$ m. Abbreviations: AD, Alzheimer's disease; SEM, standard error of the mean.

fibrin(ogen) plays a role in synaptic degeneration as well as A $\beta$  accumulation in the AD brain.

#### 4. Discussion

AD is a multifactorial disease with a vascular component, and increasing evidence suggests that fibrinogen and fibrin clot formation contribute to this disorder. Here, we further investigated the role of this plasma protein in AD pathogenesis using human post-mortem AD samples and AD mice. High levels of fibrin were found in the brains of AD patients and AD mice, and these levels appeared to correlate with the degree of A $\beta$  pathology. We also observed that fibrin(ogen) was present in areas where neurons were degenerating and losing their synapses, affecting neuronal health. These findings advance our understanding of fibrin(ogen)'s contribution to the pathophysiology of AD.

To find a therapeutic strategy aimed at normalizing the increased thrombosis present in AD, it is critical to know which are the key players as well as their localization and partners. We found that the insoluble fibrin polymer, the end point of the coagulation cascade, is abnormally present in different areas of the human AD brain intravascularly and extravascularly (Fig. 1), as well as in the

brains of AD mice where it increases over time and correlates with the level of A $\beta$  deposition (Fig. 2). Having large vessels lined with fibrin or capillaries completely blocked by its deposition (Fig. 1G–J) can alter the cerebral blood flow, especially if these vascular occlusions occur chronically over the course of many years. This could play a substantial role on the hypoperfusion present in AD patients (Austin et al., 2011; Mazza et al., 2011). Also, extravascular fibrin deposition (Fig. 1K–N) could exacerbate the chronic inflammation present in the AD brain, recruit different cells types, and promote processes such as extracellular matrix binding as well as platelet and endothelial cell spreading (Mosesson, 2005). All these events could have a deleterious effect on the brain's balanced activity.

We noticed the distribution as well as the amount of fibrin present in the brain was variable within AD patients. The AD population is very heterogeneous because different pathways are affected in this disease, which could explain why we identified only a subpopulation of AD patients with increased thrombosis. We believe this variability reinforces the fact that this disease is multifactorial and stresses the importance of developing individualized diagnosis and treatment depending on the different pathologies present in each specific AD patient.

Altered expression of postsynaptic (Gyls et al., 2004) as well as presynaptic proteins (Maslah et al., 1994) occurs in human AD patients as well as in AD mouse lines (Oakley et al., 2006). Neurodegeneration is also an important pathologic component of AD as loss of neurons occurs in multiples areas of the human AD brain (Duyckaerts et al., 2009). We report that fibrin(ogen) is present in areas packed with dystrophic neurites (Fig. 3), and more importantly, reducing fibrinogen levels increased the amount of subicular neurons by 5% (Fig. 4), decreased synaptic dysfunction by 25% (Fig. 5), and reduced amyloid pathology by more than 40% (Fig. 5). These results strongly suggest that the presence of fibrin(ogen) might be neurotoxic in this region. However, it is possible that decreasing fibrinogen levels also affects the balance of other blood- or vessel-derived proteins known to be present in microhemorrhages close to amyloid plaques (Cullen et al., 2005, 2006). Therefore, neuronal dysfunction near fibrin(ogen)-positive areas may be because of direct fibrin toxicity and/or may also be the result of a chronic vascular disease. It is possible that we did not see a bigger effect, because the reduction in plasma fibrinogen levels in these mice is only approximately 30%, and fibrin(ogen) is certainly not the only factor affecting amyloid deposition and neuronal dysfunction in AD pathology. However, even the modest 5% increase in neurons we observed because of decreasing fibrinogen levels represents approximately 300 subicular neurons/mm<sup>2</sup>, which together with the reduction in dystrophic neurites and amyloid pathology, could have a significant impact on AD progression. Because the AD brain atrophies at a rate of nearly 3% per year (Hua et al., 2013), identifying therapeutic strategies that can decrease that rate could delay disease progression considerably. Interventions with a modest interruption in disease onset and progression by 1 year could translate into avoiding 9 million AD cases by 2050 (Brookmeyer et al., 2007).

The present studies confirm the increased thrombosis present in the AD brain, which can profoundly affect brain physiology. Several factors in AD could be responsible for this increased thrombosis. Because there is an extensive cross talk between inflammation and hemostasis (Levi et al., 2004), the widespread inflammatory response present in AD (Lee et al., 2010) may lead to a procoagulant state which in turn sustains inflammation. Indeed, increased thrombin generation as well as elevated levels of activated coagulation factors and activated platelets are present in the AD circulation and brain (Cortes-Canteli et al., 2012). In addition, episodes of microhemorrhages can occur in the AD brain (Cullen et al., 2005, 2006), suggesting that blood-derived proteins, including fibrinogen, are able to cross the blood-brain barrier over long periods of time and deposit in the AD brain. Because of this prothrombotic state, it is possible that when fibrinogen extravasates into the brain, it is converted into fibrin, where it might persist, because the fibrinolytic system is reduced in the AD brain (Ledesma et al., 2000; Melchor et al., 2003). Moreover, the presence of elevated A $\beta$  in the brain would promote its binding to fibrin(ogen) (Ahn et al., 2010) and incorporate into fibrin clots, further delaying fibrinolysis (Cortes-Canteli et al., 2010; Zamolodchikov and Strickland, 2012). This fibrin deposition could then decrease cerebral blood flow, promote inflammation, and affect neuronal function, ultimately leading to cell death and cognitive deficits.

It remains to be clarified whether fibrin(ogen) deposition is a cause or a consequence of AD. High levels of fibrinogen in plasma increase the risk for dementia (Van Oijen et al., 2005; Xu et al., 2008) and fibrinogen in cerebrospinal fluid (Craig-Schapiro et al., 2011; Vafadar-Isfahani et al., 2012) and plasma (Thambisetty et al., 2011; Yang et al., 2014) has been proposed as a useful biomarker to identify AD progression. Interestingly, fibrinogen has recently been found to be one of the few blood-based biomarkers specific for AD and not for other brain disorders (Chiam et al., 2014).

However, whether fibrin(ogen) deposition and fibrin clot formation precedes or follows AD pathology is still an open question as is whether this disorder is caused by primary or secondary cerebral blood flow deficiency (Austin et al., 2011; Mazza et al., 2011). What is clear is that fibrinogen and fibrin clot formation contribute to AD pathogenesis by increasing neurovascular damage (Paul et al., 2007), neuroinflammation (Paul et al., 2007), cerebral amyloid angiopathy (Cortes-Canteli et al., 2010), and neuronal degeneration (present study). Therefore, therapeutic strategies aimed at blocking the interaction between fibrinogen and A $\beta$  (Ahn et al., 2014) or at normalizing thrombosis and decreasing the accumulation of fibrin(ogen) in the AD brain could prove useful in improving cerebral blood flow, neuronal function, and survival, which in turn could have significant long-term benefits for AD patients.

## Disclosure statement

The authors declare no conflicts of interest.

## Acknowledgements

This work was supported by the BrightFocus Foundation (grant number A2011310), NIH (grant number NS050537), Litwin Foundation, May and Samuel Rudin Family Foundation, Blanchette Hooker Rockefeller Fund, Mellam Family Foundation, and John A. Herrmann, Jr. The authors thank Drs M. Azhar Chishti and David Westaway (University of Toronto, Toronto, Canada) for providing the TgCRND8 mice, and Dr Jay L. Degen (Cincinnati, OH, USA) and Dr T. Renne (Karolinska Institutet, Sweden) for providing the fibrin(ogen) and fibrin antibodies, respectively. They thank Strickland Laboratory members for thoughtful discussions, particularly Daria Zamolodchikov for her expert advice on the detection of fibrin by Western blot and Andrew Lawson for his hard work and discussions during his summer project. They thank Jose Miguel Cortes and Shaine Abbani for technical help, and The Rockefeller University's Bio-Imaging Resource Center members for their help and support. Human brain samples were provided by the Harvard Brain Tissue Resource Center, which is supported in part by PHS (grant number R24 MH068855). Monoclonal LAMP-1 antibodies (1D4B and H4A3) developed by J. Thomas August and James E.K. Hildreth (Johns Hopkins University School of Medicine, Baltimore, MD) were obtained from the Developmental Studies Hybridoma Bank developed under auspices of the NICHD and maintained by The University of Iowa (Department of Biology, Iowa City, IA 52242).

## References

- Ahn, H.J., Glickman, J.F., Poon, K.L., Zamolodchikov, D., Jno-Charles, O.C., Norris, E.H., Strickland, S., 2014. A novel Abeta-fibrinogen interaction inhibitor rescues altered thrombosis and cognitive decline in Alzheimer's disease mice. *J. Exp. Med.* 211, 1049–1062.
- Ahn, H.J., Zamolodchikov, D., Cortes-Canteli, M., Norris, E.H., Glickman, J.F., Strickland, S., 2010. Alzheimer's disease peptide [beta]-amyloid interacts with fibrinogen and induces its oligomerization. *Proc. Natl. Acad. Sci. U. S. A.* 107, 21812–21817.
- Armstrong, A., Mattsson, N., Appelqvist, H., Janefjord, C., Sandin, L., Agholme, L., Olsson, B., Svensson, S., Blennow, K., Zetterberg, H., Kagedal, K., 2014. Lysosomal network proteins as potential novel CSF biomarkers for Alzheimer's disease. *Neuromolecular Med.* 16, 150–160.
- Austin, B.P., Nair, V.A., Meier, T.B., Xu, G., Rowley, H.A., Carlsson, C.M., Johnson, S.C., Prabhakaran, V., 2011. Effects of hypoperfusion in Alzheimer's disease. *J. Alzheimers Dis.* 26 (Suppl 3), 123–133.
- Barrachina, M., Maes, T., Buesa, C., Ferrer, I., 2006. Lysosome-associated membrane protein 1 (LAMP-1) in Alzheimer's disease. *Neuropathol. Appl. Neurobiol.* 32, 505–516.
- Brookmeyer, R., Johnson, E., Ziegler-Graham, K., Arrighi, H.M., 2007. Forecasting the global burden of Alzheimer's disease. *Alzheimer's Dement.* 3, 186–191.
- Chiam, J.T.W., Dobson, R.J.B., Kiddle, S.J., Sattlecker, M., 2015. Are blood-based protein biomarkers for Alzheimer's disease also involved in other brain disorders? a systematic review. *J. Alzheimers Dis.* 43, 303–314.

- Chishti, M.A., Yang, D.S., Janus, C., Phinney, A.L., Horne, P., Pearson, J., Strome, R., Zaker, N., Loukides, J., French, J., Turner, S., Lozza, G., Grilli, M., Kunicki, S., Morrisette, C., Paquette, C., Gervais, F., Bergeron, C., Fraser, P.E., Carlson, G.A., George-Hyslop, P.S., Westaway, D., 2001. Early-onset amyloid deposition and cognitive deficits in transgenic mice expressing a double mutant form of amyloid precursor protein 695. *J. Biol. Chem.* 276, 21562–21570.
- Condello, C., Schain, A., Grutzendler, J., 2011. Multicolor time-stamp reveals the dynamics and toxicity of amyloid deposition. *Sci. Rep.* 1, 19.
- Cortes-Canteli, M., Paul, J., Norris, E.H., Bronstein, R., Ahn, H.J., Zamolodchikov, D., Bhuvanendran, S., Fenz, K.M., Strickland, S., 2010. Fibrinogen and beta-amyloid association alters thrombosis and fibrinolysis: a possible contributing factor to Alzheimer's disease. *Neuron* 66, 695–709.
- Cortes-Canteli, M., Zamolodchikov, D., Ahn, H.J., Strickland, S., Norris, E.H., 2012. Fibrinogen and altered hemostasis in Alzheimer's disease. *J. Alzheimers Dis.* 32, 599–608.
- Craig-Schapiro, R., Kuhn, M., Xiong, C., Pickering, E.H., Liu, J., Misko, T.P., Perrin, R.J., Bales, K.R., Soares, H., Fagan, A.M., Holtzman, D.M., 2011. Multiplexed immunoassay panel identifies novel CSF biomarkers for Alzheimer's disease diagnosis and prognosis. *PLoS One* 6, e18850.
- Cullen, K.M., Kocsi, Z., Stone, J., 2005. Pericapillary haem-rich deposits: evidence for microhaemorrhages in aging human cerebral cortex. *J. Cereb. Blood Flow Metab.* 25, 1656–1667.
- Cullen, K.M., Kócsi, Z., Stone, J., 2006. Microvascular pathology in the aging human brain: evidence that senile plaques are sites of microhaemorrhages. *Neurobiol. Aging* 27, 1786–1796.
- Davalos, D., Akassoglou, K., 2012. Fibrinogen as a key regulator of inflammation in disease. *Semin. Immunopathol.* 34, 43–62.
- de la Torre, J.C., 2002. Alzheimer disease as a vascular disorder: nosological evidence. *Stroke* 33, 1152–1162.
- Duyckaerts, C., Delatour, B., Potier, M.C., 2009. Classification and basic pathology of Alzheimer disease. *Acta Neuropathol.* 118, 5–36.
- Duyckaerts, C., Potier, M.C., Delatour, B., 2008. Alzheimer disease models and human neuropathology: similarities and differences. *Acta Neuropathol.* 115, 5–38.
- Falke, E., Nisanov, J., Mitchell, T.W., Bennett, D.A., Trojanowski, J.Q., Arnold, S.E., 2003. Subicular dendritic arborization in Alzheimer's disease correlates with neurofibrillary tangle density. *Am. J. Pathol.* 163, 1615–1621.
- Fiala, M., Liu, Q.N., Sayre, J., Pop, V., Brahmandam, V., Graves, M.C., Vinters, H.V., 2002. Cyclooxygenase-2-positive macrophages infiltrate the Alzheimer's disease brain and damage the blood-brain barrier. *Eur. J. Clin. Invest.* 32, 360–371.
- Franklin, K.B.J., Paxinos, G., 2008. *The Mouse Brain in Stereotaxic Coordinates*, third ed. London, Elsevier, Amsterdam.
- Gomez-Isla, T., Price, J.L., McKeel Jr., D.W., Morris, J.C., Growdon, J.H., Hyman, B.T., 1996. Profound loss of layer II entorhinal cortex neurons occurs in very mild Alzheimer's disease. *J. Neurosci.* 16, 4491–4500.
- Gylis, K.H., Fein, J.A., Yang, F., Wiley, D.J., Miller, C.A., Cole, G.M., 2004. Synaptic changes in Alzheimer's disease: increased amyloid-beta and gliosis in surviving terminals is accompanied by decreased PSD-95 fluorescence. *Am. J. Pathol.* 165, 1809–1817.
- Hashimoto, T., Ogino, K., Shin, R.W., Kitamoto, T., Kikuchi, T., Shimizu, N., 2010. Age-dependent increase in lysosome-associated membrane protein 1 and early-onset behavioral deficits in APPSL transgenic mouse model of Alzheimer's disease. *Neurosci. Lett.* 469, 273–277.
- Hua, X., Hibar, D.P., Ching, C.R., Boyle, C.P., Rajagopalan, P., Gutman, B.A., Leow, A.D., Toga, A.W., Jack Jr., C.R., Harvey, D., Weiner, M.W., Thompson, P.M., Alzheimer's Disease Neuroimaging Initiative, 2013. Unbiased tensor-based morphometry: improved robustness and sample size estimates for Alzheimer's disease clinical trials. *Neuroimage* 66, 648–661.
- Huang, Y., Mucke, L., 2012. Alzheimer mechanisms and therapeutic strategies. *Cell* 148, 1204–1222.
- Hui, K.Y., Haber, E., Matsueda, G.R., 1983. Monoclonal antibodies to a synthetic fibrin-like peptide bind to human fibrin but not fibrinogen. *Science* 222, 1129–1132.
- Humpel, C., 2011. Chronic mild cerebrovascular dysfunction as a cause for Alzheimer's disease? *Exp. Gerontol.* 46, 225–232.
- Iadecola, C., 2010. The overlap between neurodegenerative and vascular factors in the pathogenesis of dementia. *Acta Neuropathol.* 120, 287–296.
- Jantaratnotai, N., Schwab, C., Ryu, J.K., McGeer, P.L., McLarnon, J.G., 2010. Converging perturbed microvasculature and microglial clusters characterize Alzheimer disease brain. *Curr. Alzheimer Res.* 7, 625–636.
- Jarre, A., Gowert, N.S., Donner, L., Münzer, P., Klier, M., Borst, O., Schaller, M., Lang, F., Korth, C., Elvers, M., 2014. Pre-activated blood platelets and a pro-thrombotic phenotype in APP23 mice modeling Alzheimer's disease. *Cell. Signal.* 26, 2040–2050.
- Kalaria, R.N., Akinyemi, R., Ihara, M., 2012. Does vascular pathology contribute to Alzheimer changes? *J. Neurol. Sci.* 322, 141–147.
- Klohs, J., Baltes, C., Prinz-Kranz, F., Ratering, D., Nitsch, R.M., Knuesel, I., Rudin, M., 2012. Contrast-enhanced magnetic resonance microangiography reveals remodeling of the cerebral microvasculature in transgenic ArcAbeta mice. *J. Neurosci.* 32, 1705–1713.
- Ledesma, M.D., Da Silva, J.S., Crassaerts, K., Delacourte, A., De Strooper, B., Dotti, C.G., 2000. Brain plasmin enhances APP alpha-cleavage and Abeta degradation and is reduced in Alzheimer's disease brains. *EMBO Rep.* 1, 530–535.
- Lee, S., Sato, Y., Nixon, R.A., 2011. Lysosomal proteolysis inhibition selectively disrupts axonal transport of degradative organelles and causes an Alzheimer's-like axonal dystrophy. *J. Neurosci.* 31, 7817–7830.
- Lee, Y.J., Han, S.B., Nam, S.Y., Oh, K.W., Hong, J.T., 2010. Inflammation and Alzheimer's disease. *Arch. Pharm. Res.* 33, 1539–1556.
- Levi, M., van der Poll, T., Buller, H.R., 2004. Bidirectional relation between inflammation and coagulation. *Circulation* 109, 2698–2704.
- Lipinski, B., Sajdel-Sulkowska, E.M., 2006. New insight into Alzheimer disease: demonstration of fibrin(ogen)-serum albumin insoluble deposits in brain tissue. *Alzheimer Dis. Assoc. Disord.* 20, 323–326.
- Masliah, E., Mallory, M., Hansen, L., DeTeresa, R., Alford, M., Terry, R., 1994. Synaptic and neuritic alterations during the progression of Alzheimer's disease. *Neurosci. Lett.* 174, 67–72.
- Mazza, M., Marano, G., Traversi, G., Bria, P., Mazza, S., 2011. Primary cerebral blood flow deficiency and Alzheimer's disease: shadows and lights. *J. Alzheimers Dis.* 23, 375–389.
- Melchor, J.P., Pawlak, R., Strickland, S., 2003. The tissue plasminogen activator-plasminogen proteolytic cascade accelerates amyloid-beta (Abeta) degradation and inhibits Abeta-induced neurodegeneration. *J. Neurosci.* 23, 8867–8871.
- Mosesson, M.W., 2005. Fibrinogen and fibrin structure and functions. *J. Thromb. Haemost.* 3, 1894–1904.
- Nixon, R.A., Wegiel, J., Kumar, A., Yu, W.H., Peterhoff, C., Cataldo, A., Cuervo, A.M., 2005. Extensive involvement of autophagy in Alzheimer disease: an immunoelectron microscopy study. *J. Neuropathol. Exp. Neurol.* 64, 113–122.
- O'Mara, S., 2005. The subiculum: what it does, what it might do, and what neuroanatomy has yet to tell us. *J. Anat.* 207, 271–282.
- Oakley, H., Cole, S.L., Logan, S., Maus, E., Shao, P., Craft, J., Guillozet-Bongaarts, A., Ohno, M., Disterhoft, J., Van Eldik, L., Berry, R., Vassar, R., 2006. Intraneuronal beta-amyloid aggregates, neurodegeneration, and neuron loss in transgenic mice with five familial Alzheimer's disease mutations: potential factors in amyloid plaque formation. *J. Neurosci.* 26, 10129–10140.
- Paul, J., Strickland, S., Melchor, J.P., 2007. Fibrin deposition accelerates neurovascular damage and neuroinflammation in mouse models of Alzheimer's disease. *J. Exp. Med.* 204, 1999–2008.
- Perez-Gracia, E., Torrejon-Escribano, B., Ferrer, I., 2008. Dystrophic neurites of senile plaques in Alzheimer's disease are deficient in cytochrome c oxidase. *Acta Neuropathol.* 116, 261–268.
- Prince, M., Jackson, J., 2009. *World Alzheimer Report 2009. Alzheimer's Disease International*, London, pp. 1–93.
- Ryu, J.K., McLarnon, J.G., 2009. A leaky blood-brain barrier, fibrinogen infiltration and microglial reactivity in inflamed Alzheimer's disease brain. *J. Cell. Mol. Med.* 13, 2911–2925.
- Schindler, J., Jung, S., Niedner-Schatteburg, G., Friauf, E., Nothwang, H.G., 2006. Enrichment of integral membrane proteins from small amounts of brain tissue. *J. Neural Transm.* 113, 995–1013.
- Selkoe, D.J., 2011. Alzheimer's disease. *Cold Spring Harb. Perspect. Biol.* 3, a004457.
- Solito, E., Sastre, M., 2012. Microglia function in Alzheimer's disease. *Front. Pharmacol.* 3, 14.
- Suh, T.T., Holmback, K., Jensen, N.J., Daugherty, C.C., Small, K., Simon, D.I., Potter, S., Degen, J.L., 1995. Resolution of spontaneous bleeding events but failure of pregnancy in fibrinogen-deficient mice. *Genes Dev.* 9, 2020–2033.
- Tabrizi, P., Wang, L., Seeds, N., McComb, J.G., Yamada, S., Griffin, J.H., Carmeliet, P., Weiss, M.H., Zlokovic, B.V., 1999. Tissue plasminogen activator (tPA) deficiency exacerbates cerebrovascular fibrin deposition and brain injury in a murine stroke model: studies in tPA-deficient mice and wild-type mice on a matched genetic background. *Arterioscler. Thromb. Vasc. Biol.* 19, 2801–2806.
- Terry, R.D., Masliah, E., Salmon, D.P., Butters, N., DeTeresa, R., Hill, R., Hansen, L.A., Katzman, R., 1991. Physical basis of cognitive alterations in Alzheimer's disease: synapse loss is the major correlate of cognitive impairment. *Ann. Neurol.* 30, 572–580.
- Thambisetty, M., Simmons, A., Hye, A., Campbell, J., Westman, E., Zhang, Y., Wahlund, L.O., Kinsey, A., Causevic, M., Killick, R., Kloszewska, I., Mecocci, P., Soininen, H., Tsolaki, M., Vellas, B., Spenger, C., Lovestone, S., 2011. Plasma biomarkers of brain atrophy in Alzheimer's disease. *PLoS One* 6, e28527.
- Vafadar-Isfahani, B., Ball, G., Coveney, C., Lemetre, C., Boocock, D., Minthon, L., Hansson, O., Miles, A.K., Janciauskiene, S.M., Warden, D., Smith, A.D., Wilcock, G., Kalsheker, N., Rees, R., Matharoo-Ball, B., Morgan, K., 2012. Identification of SPARC-like 1 protein as part of a biomarker panel for Alzheimer's disease in cerebrospinal fluid. *J. Alzheimers Dis.* 28, 625–636.
- van Oijen, M., Witteman, J.C., Hofman, A., Koudstaal, P.J., Breteler, M.M., 2005. Fibrinogen is associated with an increased risk of Alzheimer disease and vascular dementia. *Stroke* 36, 2637–2641.
- Viggars, A.P., Wharton, S.B., Simpson, J.E., Matthews, F.E., Brayne, C., Savva, G.M., Garwood, C., Drew, D., Shaw, P.J., Ince, P.G., 2011. Alterations in the blood brain barrier in ageing cerebral cortex in relationship to Alzheimer-type pathology: a study in the MRC-CFAS population neuropathology cohort. *Neurosci. Lett.* 505, 25–30.
- Weisel, J.W., 2005. Fibrinogen and fibrin. *Adv. Protein Chem.* 70, 247–299.
- Wirhlich, O., Bayer, T.A., 2010. Neuron loss in transgenic mouse models of Alzheimer's disease. *Int. J. Alzheimers Dis.* 2010 pii: 723782.
- Xu, G., Zhang, H., Zhang, S., Fan, X., Liu, X., 2008. Plasma fibrinogen is associated with cognitive decline and risk for dementia in patients with mild cognitive impairment. *Int. J. Clin. Pract.* 62, 1070–1075.
- Yang, H., Lyutvinskiy, Y., Herukka, S.K., Soininen, H., Rutishauser, D., Zubarev, R.A., 2014. Prognostic polypeptide blood plasma biomarkers of Alzheimer's disease progression. *J. Alzheimers Dis.* 40, 659–666.
- Zamolodchikov, D., Strickland, S., 2012. Abeta delays fibrin clot lysis by altering fibrin structure and attenuating plasminogen binding to fibrin. *Blood* 119, 3342–3351.
- Zilkova, M., Koson, P., Zilka, N., 2006. The hunt for dying neurons: insight into the neuronal loss in Alzheimer's disease. *Bratisl. Lek. Listy* 107, 366–373.